Lava flow surface roughness and depolarized radar scattering

Bruce A. Campbell

Center for Earth and Planetary Studies, Smithsonian Institution, Washington, D.C.

Michael K. Shepard

Department of Geography and Earth Science, Bloomsburg University, Bloomsburg, Pennsylvania

Abstract. Surface roughness has a strong controlling influence on radar scattering and other types of remote sensing observations. We compare field measurements of surface topography and dielectric constant for a range of lava flow textures to aircraft multipolarization radar observations at 5.7, 24, and 68 cm (C, L, and P band) wavelengths. The roughness is found to vary with scale in a self-affine (fractal) manner for scale lengths between 25 cm (the smallest horizontal step size) and 3-5 m. This result is used to demonstrate that a two-component surface description, consisting of the fractal dimension and rms height or slope at some reference scale, can resolve some of the ambiguities in previous efforts to quantify roughness. At all three radar wavelengths, the HV backscatter cross section is found to vary in an approximately exponential fashion with the rms height or Allan deviation at some reference scale, up to a saturation point, where the surface appears entirely diffusely scattering to the radar. Based on these observations, we use a parameter, γ, defined as the ratio of rms height to the particular scale of measurement. Backscatter values at 24-cm wavelength and the topographic profile data were used to derive expressions which link the HV radar cross section to γ or to the analogous wavelength-scale rms slope. These equations provide a reasonable fit to 24- and 68-cm echoes and for rough surfaces at 5.7 cm, but yield poor results for 5.7-cm echoes on smooth terrain. We conclude that the roughness at the two larger scales is well described by a single fractal dimension and rms height, but that texture at very small scales is characterized by different statistics. This inference is supported by analysis of 5-cm horizontal spacing topographic profiles. The relationships defined here allow determination of the surface rms height or slope at the scale of the radar wavelength. Given radar data at additional wavelengths, a more complete view of the statistical properties of the surface can be developed. Such techniques may be useful in analyses of synthetic aperture radar images for terrestrial volcanic areas, Magellan data for Venus, and other planetary radar observations.

Introduction

The topography of natural surfaces at scales of a few meters or less is commonly referred to as roughness. These variations in height and slope, their magnitude, and the changes in structure as a function of scale length are of fundamental importance to the interpretation of geologic emplacement mechanisms and subsequent modification. For most planetary studies and many terrestrial situations, no in situ observations of the ground are available, and remote sensing data are used to infer the nature of the terrain. For optical, infrared, and microwave measurements, surface roughness and its scale dependence have a large impact on the brightness, polarization, angular scattering properties, and wavelength dependence of reflected and emitted energy. The link between

surface roughness and specific remote sensing properties for many types of observations remains elusive. In this paper, we focus on the nature of roughness and its scale dependence for terrestrial rocky lava surfaces, and the effect of such changes on depolarized radar backscatter at a variety of incidence angles and wavelengths.

Analysis of radar scattering from natural surfaces has been of interest for over 30 years, and two distinct approaches have been followed. The first involves development of tractable analytical expressions for the scattered field from surfaces with well-defined statistical properties, permitting direct prediction of roughness from observed radar echoes. The most successful of these models are those proposed by *Hagfors* [1964] for echoes at very small incidence angles, and the small-perturbation model, developed by a number of workers [e.g., *Barrick and Peake*, 1967]. The mathematical restrictions on roughness required by analytical models may not be satisfied by a target surface, such as was found in a comparison of the radar polarization properties of lava flows and playa surfaces to predictions of the first-order small-perturbation

model [*Campbell et al.*, 1993]. For some models, adjustments to the data for other scattering effects are needed; the use of a diffuse scattering correction for Venus reflectivity data is a good example [*Pettengill et al.*, 1988].

A second approach to the problem has been direct measurement of surface roughness for various field sites, and comparison of these data to available radar images. Techniques for surface measurement range from production of stereo models from photographs to direct surveying. Such methods have been used in numerous studies of radar backscatter [e.g., *Schaber et al.*, 1976, 1980; *Ulaby et al.*, 1982; *Campbell et al.*, 1989; *van Zyl et al.*, 1991; *Farr*, 1992; *Oh et al.*, 1992; *Gaddis et al.*, 1990; *Gaddis*, 1992, 1994; *Arvidson et al.*, 1993; *Campbell and Garvin*, 1993; *Benallegue et al.*, 1995]. Analysis of field roughness measurements is, however, complicated by the question of scale dependence for statistical parameters such as rms height, rms slope, and correlation length. These parameters appear as variables in many radar scattering models, but the surface scales to which they apply is often poorly defined.

This paper examines a combination of topographic and radar scattering information for 10 sites on Kilauea Volcano in Hawaii. We first quantify the effect of changing horizontal scale on roughness parameters, examine basic issues in sampling and characterizing natural surfaces, and suggest descriptors which may be useful in comparing data from different experiments. Next, the behavior of depolarized radar backscatter on surface structure is analyzed, and a model is

developed which relates the HV radar cross section to dimensionless roughness parameters. Finally, we discuss applications and future directions for this work.

Topographic and Radar Data

The topographic data used here were collected by three techniques. The majority of the Kilauea profiles used a surveying level and a stadia rod to define vertical offsets, and a taut line marked at 25-cm intervals to measure horizontal spacing. The vertical accuracy is typically 1 cm (the smallest gradation on the rod), while the horizontal accuracy is limited by the degree to which the line lies parallel to the ground. Later surveys were carried out with a PulseRanger laser rangefinder, which has a horizontal accuracy over long baselines of about ±5 cm. Profile lengths are 80-120 m, and are shown in Figure 1. A more limited set of high-resolution (5-cm spacing) profiles was collected using a laser rangefinder on a horizontal trestle [*Campbell and Garvin*, 1993].

The radar data were collected in 1990 by the NASA/Jet Propulsion Laboratory airborne synthetic aperture radar (AIRSAR) system, which uses orthogonal linear-polarized antennas to acquire the full Stokes matrix information for each resolution cell [*Evans et al.*, 1986]. Images for radar wavelengths of 5.7, 24, and 68 cm (C, L, and P band) are obtained simultaneously. Calibration is checked against corner reflector targets within the scene whose scattering properties and orientations are known [*Freeman et al.*, 1992;
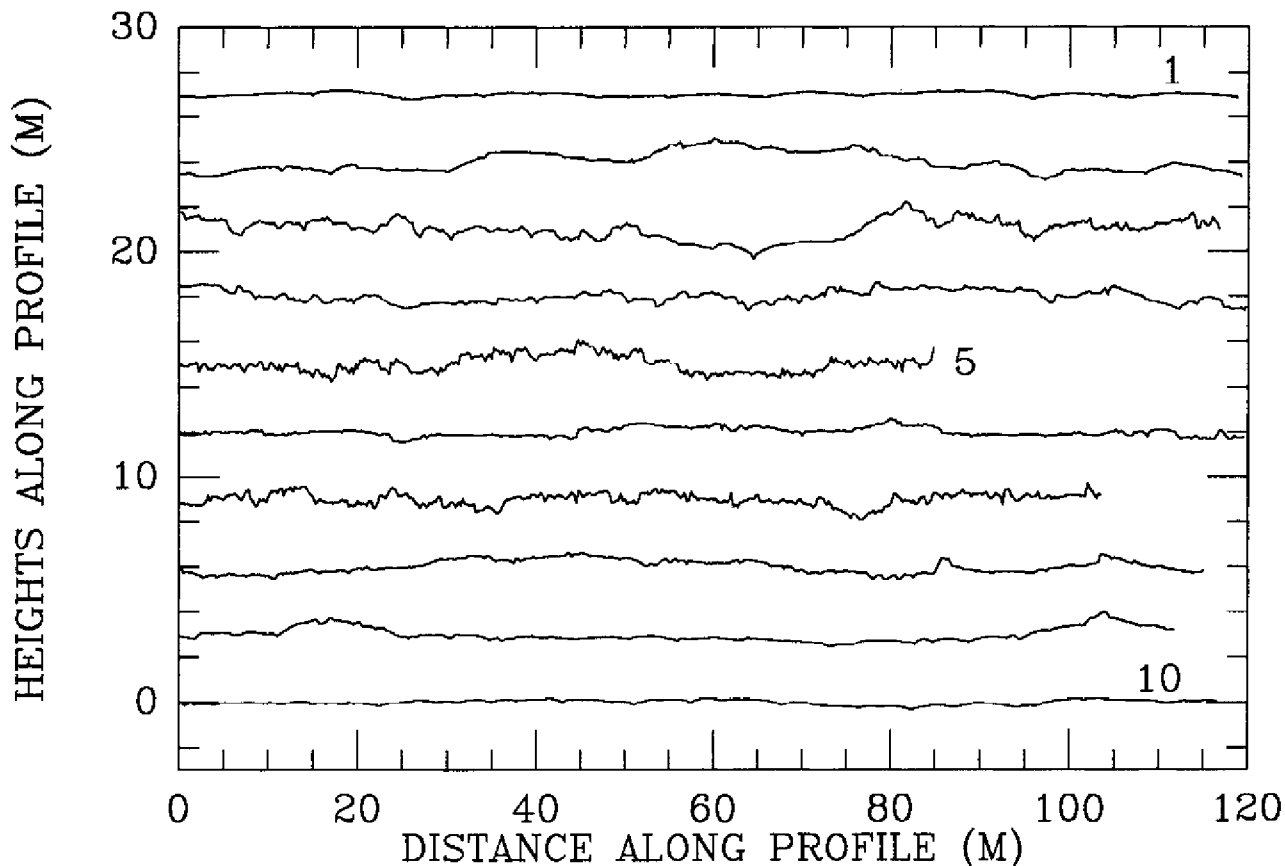

Figure 1. Topographic profiles for 10 study sites on Kilauea Volcano, Hawaii. Horizontal step size is 25 cm. Each profile has been detrended by removal of a best fit straight line, and offset by an arbitrary amount for clarity. Site numbers correspond to those in Figure 2.

Plate 1. Radar image of Kilauea Caldera and Kau Desert study area. The 5.7-, 24-, and 68-cm HV echoes are coded as red, green, and blue channels, respectively. Image has been geometrically corrected to 10-m ground pixels. Image width 18 km. A'a flows appear as bright yellow or white, smooth pahoehoe surfaces are dark red, and vegetation near the caldera is white.

van Zyl, 1990]. The absolute calibration reliability of these data is of the order of 1-2 dB, but within a scene the relative shifts in power between different surfaces can be defined even more accurately. A composite image of Kilauea at three radar wavelengths is shown in Plate 1.

The field sites on Kilauea were chosen to illustrate the range of surface roughness at scales below about one meter, and the locations of these sites are noted in Figure 2. The smoothest surfaces are those formed by ponding of lava in topographic depressions, represented by portions of the 1974 and 1982
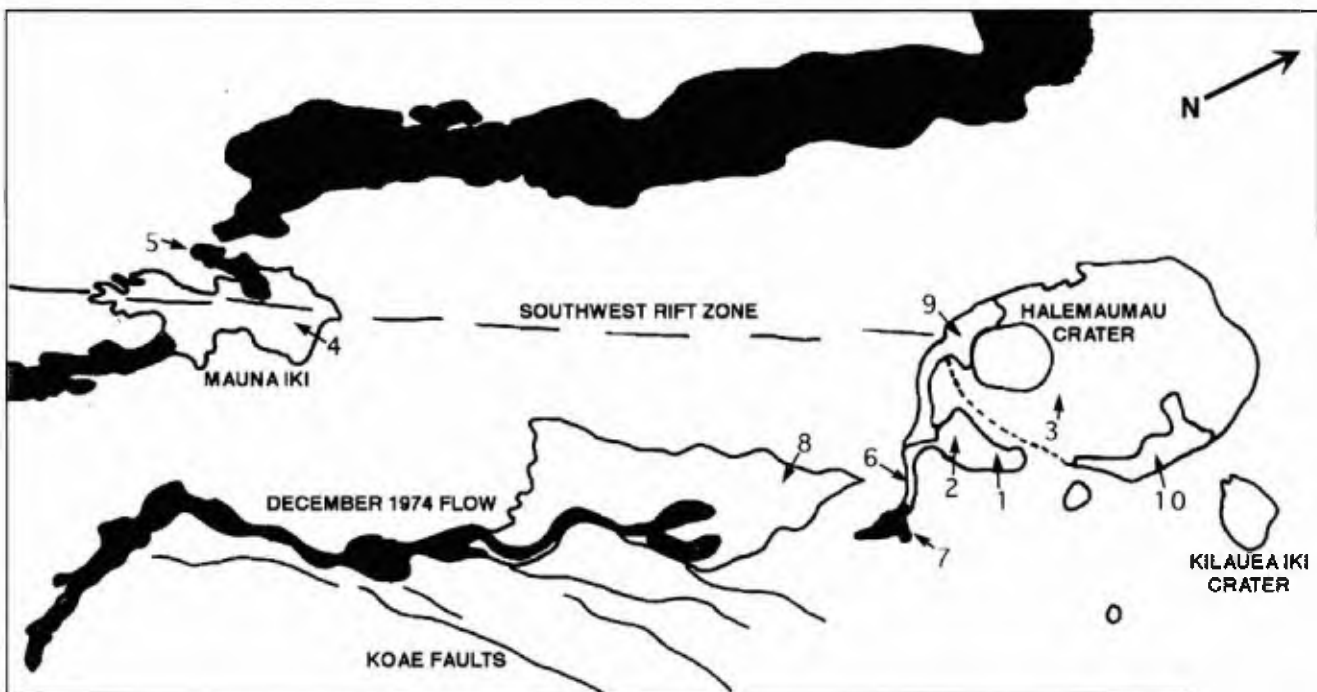

Figure 2. Sketch map of major Kilauea summit/Kau desert flow units and topographic site locations. A'a flow units shown by gray shading.
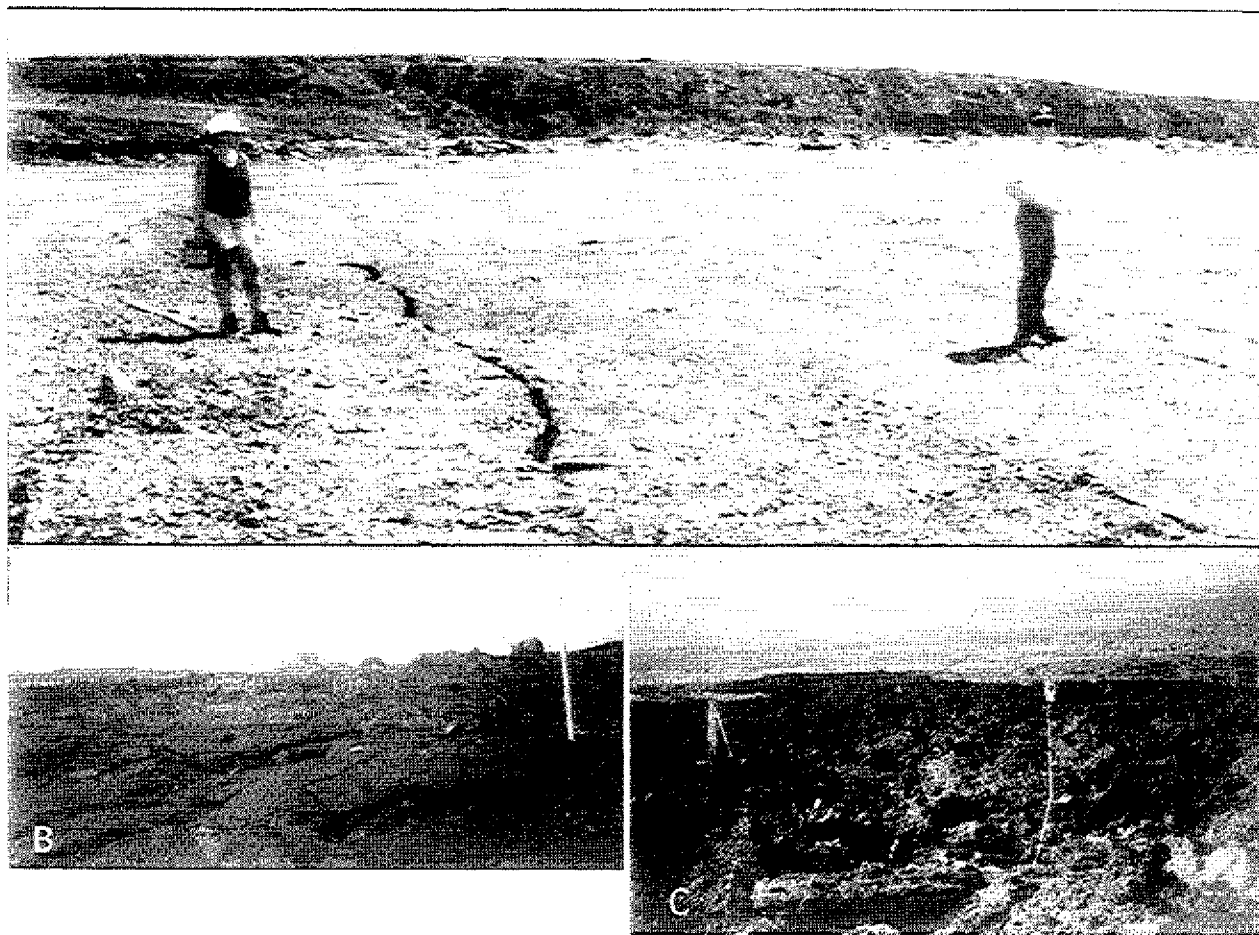
Figure 3. Photographs of representative field sites on Kilauea. (a) Ponded pahoehoe (site 1). The small-scale texture consists of small chips of broken surface glass. (b) Pahoehoe flow with larger billows and toes (site 3). Pole is approximately 1.5 m in height. (c) A'a flow (site 5).

flows. These areas are typically composed of large plates of basalt, 2-5 m in extent, which are flat or slightly curved (Figure 3a). Increasing roughness is found on pahoehoe flows which traveled down a slope without ponding. The surface of these flows is characterized by toes, billows, plates, and ropes of varying magnitude and distribution (Figure 3b). Pahoehoe flows are generally associated with a combination of lower magma viscosity and small local flow rates [*Rowland and Walker*, 1990]. As the combination of flow rate and viscosity passes some critical threshold, the surface of the lava no longer seals cracks and begins to develop spiny or blocky texture characteristic of a'a morphology. These flows represent the roughest Hawaiian basalt terrains, and several are included among the field sites (Figure 3c).

Statistical Descriptions of Surface Roughness

The role of surface roughness variations in radar backscatter, optical shadowing, thermal emission, and other remote sensing measurements has long been recognized. Methods for quantifying small-scale topography are rarely consistent between different experiments, however, and the relevance of any given parameter to scattering or emission at the observing wavelength is difficult to assess. In this section, we examine several parameters for surface characterization, assess the role of horizontal measurement scale in determining the value of each, and offer a synthesis which may permit more direct comparison of remote observations and measured topographic information. The two parameters most often used in surface descriptions, radar scattering models, and optical shadowing estimates are the root-mean-square (rms) height (h_o) and the rms slope ($s=\tan\theta$).

The rms Height

In general, surface topography data are analyzed in the form of profiles collected along a fixed line, so we focus here on this type of data. The rms height is calculated as the standard deviation of vertical offsets along the profile, but several complicating factors must be considered in deriving and using this parameter [*Shepard et al.*, 1995]. These issues include the length of the profile and whether a trend line is removed. As the profile length is increased, the rms height will also increase; if we shorten the profile, the rms height will decrease. This can be seen identically from two viewpoints: one based on the Fourier transform approach to surface description, and the other based on fractal methods. For the Fourier case, increasing the profile length corresponds to sampling more of the long-wavelength component of the surface. For many natural surfaces, the range of heights tends to be larger over greater distances, so h_o rises as we consider

these components. Shortening the profile is analogous to a high-pass filtering operation. *Campbell and Garvin* [1993] noted these properties in a study of three lava surfaces, but Fourier methods offer no simple way to express the change in h_0 with measurement scale.

Recently, scale-dependence problems in many fields have been addressed using self-affine or fractal descriptors. The fractal dimension D, in particular, can provide a powerful measure of the change in surface roughness as a function of measurement scale. One method of defining this parameter is based upon the slope of a plot of $\log(L)$ versus height variance $\log(h_0^2(L))$, where L is the effective horizontal profile length obtained by high-pass filtering the raw topographic data. In this case, the slope of the plot equals $2(2-D)$. A self-affine or fractal surface is characterized by rms height values which scale multiplicatively with shifts in horizontal scale length. While an ideal fractal would carry this behavior through all possible length scales, we utilize the relationship only over some finite range of scales which are relevant to the landform or process under study. If the surface behaves, over some range of scales, in a self-affine manner, then we can describe the rms height with only two parameters

$$h_o(L) = C\,L^{2-D} \qquad (1)$$

where C is a constant which expresses the relative roughness magnitude of the surface. This makes the rms height very sensitive to the method of data collection and analysis, since profiles with different lengths will yield quite different descriptive values if not filtered to the same scale [*Shepard et al.*, 1995]. By using a high-pass filter with a cutoff wavelength L, we can remove the issue of profile length by essentially producing a series of segments of this characteristic length. Longer profiles simply generate a larger number of independent samples of these short segments.

Most authors "detrend" profile measurements, by removing a best fit linear function, as part of the preliminary data reduction [e.g., *Ulaby et al.*, 1982; *Gaddis et al.*, 1990; *Campbell and Garvin*, 1993]. In strict terms this biases the variogram at longer spatial scales toward lower estimates of the fractal dimension, but this assumes that the larger scales are in fact relevant to the surface study. For the lava flows studied here, the underlying trend surface represents primarily the slope of the original terrain and, as such, was not formed by the same process which created the lava texture. While this rationale could be carried to higher orders of polynomial fits or other trend-removal algorithms, first-order detrending seems reasonably justified in the context of radar scattering or optical shadowing studies. This correction ignores shifts in the local incidence angle caused by regional tilts, but in all cases the slope changes were relatively small, and the depolarized radar backscatter varies only slowly with angle.

The rms Slope

The rms slope has been variously defined as either the standard deviation of slope between successive profile points (unidirectional slope), the standard deviation of maximum local slope at each point (adirectional slope), or the ratio of rms height to correlation length [e.g., *Hagfors*, 1964; *McCollom and Jakosky*, 1993; *Campbell and Garvin*, 1993]. This parameter has been most widely used in Hagfors' model for quasi-specular scattering and in optical shadowing derivations [e.g., *Hapke*, 1984; *Smith*, 1967; *Wagner*, 1966].

We use the terminology common to many of these authors, with rms slope denoted by s, or equivalently, $\tan\theta$.

The definition of rms slope as the ratio (h_0/d_0), where d_0 is the correlation length, is applicable only for surfaces with no roughness at scales smaller than the shortest wavelength relevant to the scattering problem. If there is significant small-scale roughness (a common feature of natural surfaces), then the correlation function will have a complicated shape near the origin, and the derived value of d_0 is not a reliable indicator of correlation at any one scale [*Hagfors*, 1964]. This ratio is more often calculated from model fits to measured backscatter, then used to infer the magnitude of roughness at the scales which dominate the scattering process. Efforts to predict near-nadir scattering from a single value of (h_0/d_0) derived from a surface profile are likely to be unreliable, since both parameters will vary with the fractal dimension and measurement scale [*Shepard et al.*, 1995].

Use of an adirectional slope distribution more closely follows the definition of rms slope suggested by Hagfors in the quasi-specular scattering model, which is predicated on echoes from facets perpendicular to the incident wave [*McCollom and Jakosky*, 1993]. Such slope measurements will have a Rayleigh distribution, whereas the unidirectional slope distribution is Gaussian [*Shepard et al.*, 1995]. Field data collection for this type of estimate requires either measurement of a grid of elevations to define true slopes, or estimates of the maximum local slope at points along a profile line. The main drawback of the second method is that no surface scale can be defined except the length over which each slope is measured. As such, the role of high-frequency components on local slopes cannot be determined, and any inference of a meaningful value for s is difficult.

The rms slope determined from the distribution of tilts between profile points can be linked to the measurement scale through the Allan deviation:

$$\nu(\Delta x) = \left\langle [h(x) - h(x+\Delta x)]^2 \right\rangle^{0.5} \qquad (2)$$

where $h(x)$ are the heights at each profile point and Δx is a chosen horizontal separation. The Allan variance, used to form variogram plots, is simply $\nu^2(\Delta x)$. The ratio $\nu(\Delta x)/\Delta x$ is the rms slope s ($\tan\theta$) at a horizontal scale of Δx, and this parameter has several advantages relative to the rms height: (1) it is independent of profile length for any given step size, where h_0 requires normalization or filtering to account for L, (2) it can be defined down to the smallest measured profile step size, whereas h_0 cannot be defined for very short profile segments. For a self-affine surface, the Allan deviation varies with fractal dimension D as

$$\nu(\Delta x) = C\Delta x^{2-D} \qquad (3)$$

We can thus use the slope of the log-log variogram plot as a second method for estimating the fractal dimension of a surface.

Analysis of Topographic Profiles

For each study site (Figure 1), we calculated the variogram function using methods reviewed by *Shepard et al.* [1995] and found the best fit value of D for scales <1 m and >1 m. Examples of these variograms for a range of surface roughness are shown in Figure 4, and illustrate several common features. At scales between 25 cm and 2-5 m, the log-log plot of Allan variance versus Δx is linear, with inferred D values which vary
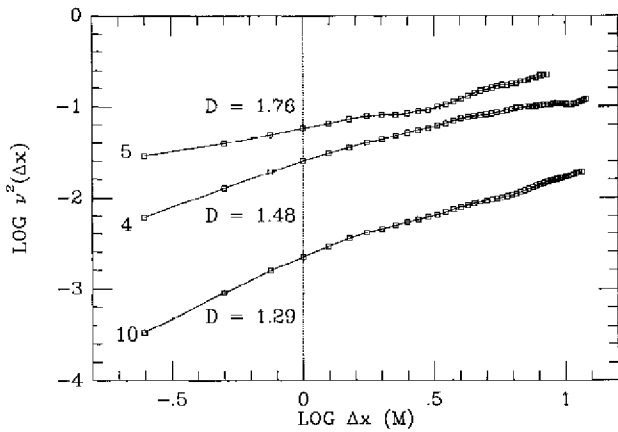
Figure 4. Variogram plots for representative sample sites. Site numbers correspond to those in Figure 2. The dashed line indicates a scale length of 1 m, and best-fit fractal dimensions for each flow at scales <1 m are noted. The change in behavior at scales of 2-5 m may be due to poor sampling of long-wavelength topography by the profiles.

from 1.3 to 1.7 (Table 1); a D value of 1.5 is consistent with ordinary Brownian noise or a "random walk" process. At larger scales the plot may roll off or oscillate, which may reflect the poor sampling of topography at several-meter scales by profiles which are only 80-120 m long. As expected, removal of a first-order trend affected the variogram only in the long-wavelength region, and we have used only detrended data here. The lava flow surfaces display self-affine behavior at scales below a few meters, and the fractal dimension and rms height (1) or rms slope (3) at a reference scale can be used to provide a robust two-component model for surface roughness. This is analogous to using the power spectral density function slope and offset [van Zyl et al., 1991] but with greater ease of physical interpretation.

The above results demonstrate how to estimate descriptive surface parameters from a profile at any scale for which the fractal behavior applies. If we use a high-pass filter to obtain profiles with a length L_0 (analogous to subdividing the long profile into smaller segments of fixed length) then we may predict the rms height at any other scale L for which we believe the self-affine scaling relationship holds:

$$h_a(L) = h_a(L_o)\left[\frac{L}{L_o}\right]^{2-D} \qquad (4)$$

A similar relationship can be obtained for the rms slope, but now the determining value is the horizontal step size, such that a measurement of s at a scale Δx_0 can be extrapolated to other step sizes:

$$s(\Delta x) = \tan\theta(\Delta x) = s(\Delta x_o)\left[\frac{\Delta x_o}{\Delta x}\right]^{2-D} \qquad (5)$$

For random-walk surfaces ($D=1.5$), the dependence on surface scale thus has a square-root form. Roughness will not generally exhibit a single self-affine behavior over all horizontal scales, and changes in scale-dependence may be linked to differences in the formational mechanisms of surface features at varying length scales. In the next section, we examine radar scattering from Hawaiian lava flows and its correlation with roughness at a range of scales.

Analysis of Diffuse Radar Scattering

The Kilauea field area was covered by three overlapping flight lines which acquired radar images at three incidence angles for each point on the ground. For each field site (Figure 2), we averaged the radar backscatter values in a rectangular box. Since the AIRSAR data for different flight lines are not coregistered, and vary in their range resolution as a function of incidence angle, the specific terrain included within the boxes for all three scenes will vary slightly. The topographic sites were chosen in areas of relatively homogeneous structure, so it is expected that the backscatter values are representative. Using the Stokes matrix information, we synthesized HH, VV, LR, LL, and HV backscatter cross section (σ^0) values at 5.7, 24, and 68 cm wavelengths (for each combination, the first letter refers to the transmitted polarization, while the second refers to the received sense: H, V, L, and R are horizontal, vertical, left-circular, and right circular).

Radar scattering is often described as the sum of two mechanisms: a quasi-specular component from large radar-facing facets, and a diffuse component due to scatterers on the scale of the incident wavelength [Hagfors, 1964, 1967]. Such a model was shown to fit the scattering from Kilauea lava flows at 5.7- and 24-cm wavelengths, with the assumption that the quasi-specular echo at high incidence angles arose from facets which must be relatively small [Campbell et al., 1993]. The diffuse component exhibited polarization

Table 1. Values of the Fractal Dimension D, rms Height h_0 at 1 m Profile Length, and the Allan Deviation v at 25, 75, and 100-cm Step Sizes for Kilauea Field Sites

Site	D (<1 m)	D (>1m)	h_0 (1 m)	v(25 cm)	v(75 cm)	v(1 m)
1	1.47	1.30	0.70	1.75	3.15	3.89
2	1.36	1.30	1.49	4.14	8.39	10.30
3	1.47	1.50	4.05	10.46	18.77	21.36
4	1.48	1.51	3.43	7.70	13.73	15.65
5	1.76	1.74	7.94	16.91	22.01	23.93
6	1.54	1.60	2.21	5.33	8.89	10.00
7	1.65	1.70	5.93	14.07	20.66	21.68
8	1.48	1.54	2.04	5.51	9.61	10.80
9	1.31	1.42	1.18	3.54	7.49	9.01
10	1.29	1.61	0.55	1.82	3.96	4.78

All h_0 and v values are in units of centimeters. D values were derived from the slope of a variogram plot, and were calculated separately for scales above and below 1 m.
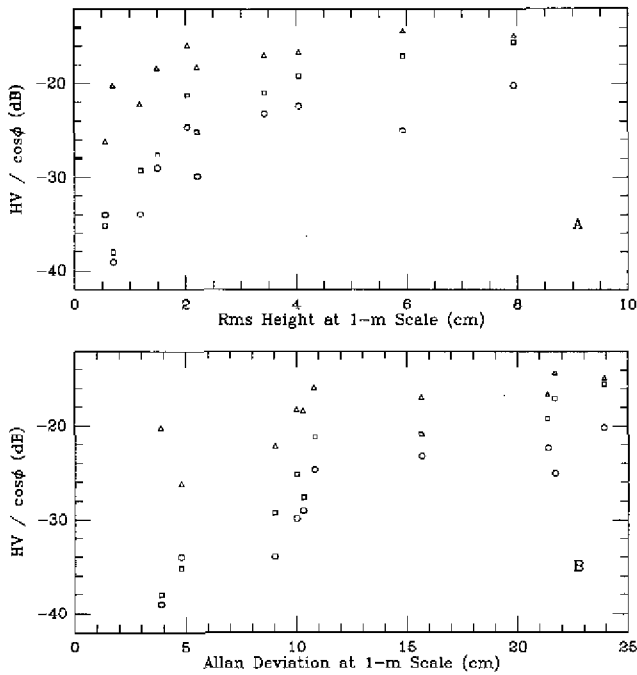
Figure 5. Plots of normalized HV backscatter power (in dB) versus roughness parameters rms height and Allan deviation at 1-m scale. Triangles indicate 5.7-cm data, squares are 24-cm values, and circles are 68-cm backscatter. (a) Backscatter versus rms height, h_0. (b) Backscatter versus Allan deviation, v.

$$\gamma = \frac{h_0(\lambda)}{\lambda} \qquad (6)$$

This is linked to the measured rms height at a reference scale λ_0 (i.e., profile length) by (4), such that

$$\gamma = \frac{h_0(\lambda_o)}{\lambda_0^{2-D}} \lambda^{1-D} \qquad (7)$$

where D is the fractal dimension of the surface. A similar parameter can also be defined in terms of the ratio $v(\lambda)/\lambda$; this is the rms slope s at a horizontal step size (Δx) equal to the radar wavelength. In the following, we will use γ only with reference to the rms height (6), and s (tan θ) for the wavelength-scale rms slope value derived from the Allan deviation. The two values are related by the nature of the surface autocorrelation function, so an analytical link cannot be made except for certain special cases (e.g., Gaussian or exponential autocorrelation behaviors).

Similar scaling parameters are commonly found in Mie theory, other optical scattering expressions, and more specifically in the Rayleigh criteria for radar scattering. *Beckmann and Spizzichino* [1963] proposed the use of the h_0/λ parameter, which they called g, to characterize the effect of roughness on the scattered power in the specular lobe of a Gaussian surface. Complications arise, however, when one considers the scale at which the rms height is defined. In their application, the scattering envelope is defined by both the g parameter and the correlation length, analogous to our use of rms height and fractal dimension to describe surface roughness. The two approaches parallel one another, but the self-affine surface descriptors provide a simpler way of relating measured profile data to observed backscatter. The parameters γ and s are based on the specific requirement that the rms height or slope be defined at a surface scale equal to the observing wavelength.
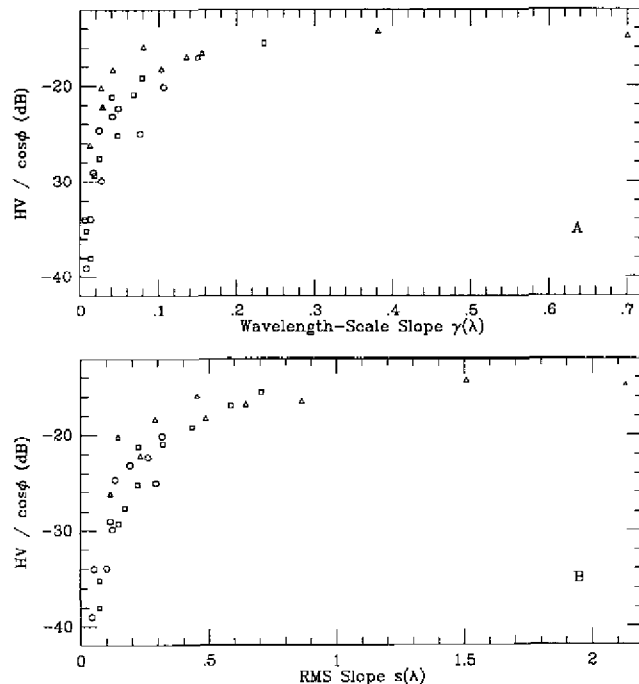
properties consistent with those of a field of randomly oriented small dipole scatterers (cracks, edges). Given the reasonable intuitive link between small-scale roughness and diffuse scattering, we chose to study this echo component first. All of the returned power in the depolarized linear sense is assumed to arise from diffuse scattering, so the HV value is used as a measure of this component. The HV power was further normalized to the cosine of the incidence angle, since this represented a good approximation to the typical angular scattering behavior of each site. This normalization permitted us to average all of the backscatter observations to a single value for each test area.

At all three wavelengths, there is an approximately exponential dependence of HV power on h_0 (Figure 5a) and v at a reference scale of 1 m (Figure 5b). For the 5.7-cm data, σ^0 appears to approach an asymptotic value at higher roughness. We infer that surfaces reach a saturation point beyond which further increases in the roughness do not change the distribution of power, and the backscatter return stays relatively constant. While the functional behavior is similar for 5.7-, 24-, and 68-cm data, there is still a significant separation between echoes at different wavelengths for a given value of h_0 or v, demonstrating that diffuse scattering is linked to a scaling relationship between roughness and λ.

Since there are no analytical scattering models for echoes from small irregular objects, we begin with the simple assumption that diffuse scattering is related to the ratio between surface roughness at the wavelength scale and the illuminating wavelength. A new parameter which expresses the relative magnitudes of the surface roughness and the illuminating wavelength, λ, is defined as

Figure 6. Plots of normalized HV backscatter power (in dB) versus roughness parameters γ and s. Triangles indicate 5.7-cm data, squares are 24-cm values, and circles are 68-cm backscatter. (a) Backscatter versus γ. (b) Backscatter versus s.

If the normalized backscatter coefficients for our field sites are plotted against these parameters (Figure 6) it is evident that, because the data cluster along a common curve, a single functional form may be used to express the scattering at all three wavelengths. We explored a variety of functional forms which could match the observed dependence of diffuse backscatter on the roughness parameters, but only one appears to offer the proper behavior, such that

$$\sigma^0_{HV}(\gamma) = 0.04 \cos\phi \, (1 - e^{-60\gamma^2}) \qquad (8)$$

$$\sigma^0_{HV}(s) = 0.04 \cos\phi \, (1 - e^{-1.7s^2}) \qquad (9)$$

where ϕ is the radar incidence angle. The fit to $\sigma^0(\gamma)$ was derived using 24-cm (L band) radar data, with height values interpolated from $h_0(1$ m) and D ((4), Table 1). The L band data were chosen since at this scale we have the best match between measured roughness and backscatter (P band data have such low cross sections on smooth surfaces that a fit would be more questionable). The fit to $\sigma^0(s)$ used the same radar measurements and values of the Allan variance calculated from the raw profile (25-cm spacing) data. The advantage of this method is that we required no fractal dimension to interpolate to the 24-cm scale.

These relationships can be inverted to yield an estimate of h_0 or s at the wavelength scale from any HV radar observation:

$$h_0(\lambda) = \lambda \left[-\frac{1}{60} \ln \left(1 - \frac{\sigma^0_{HV}}{0.04\cos\phi} \right) \right]^{0.5} \qquad (10)$$

$$s(\lambda) = \left[-\frac{1}{1.7} \ln \left(1 - \frac{\sigma^0_{HV}}{0.04\cos\phi} \right) \right]^{0.5} \qquad (11)$$

Note that these expressions do not depend upon the fractal dimension; we are simply assuming that the relationship between γ or s and σ^0 holds over a range of radar wavelengths. If HV backscatter values are available at other wavelengths,
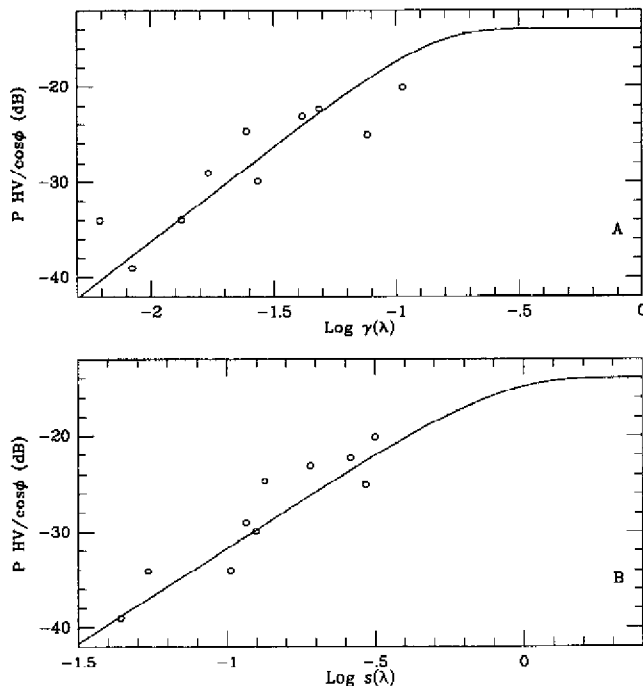

Figure 7. Normalized 68-cm HV radar data plotted against roughness parameters, with fit from model equations shown by solid line. (a) Backscatter power versus γ, with model fit from (8). (b) Backscatter power versus s, with model fit from (9).

Figure 8. Normalized 24-cm HV radar data plotted against roughness parameters, with fit from model equations shown by solid line. (a) Backscatter power versus γ, with model fit from (8). (b) Backscatter power versus s, with model fit from (9).

then in theory one could derive a fractal dimension from the variation in h_0 or s with λ through (4) and (5).

The model represented by (8) and (9) has an asymptotic behavior as roughness increases. For very large values of γ or s, the backscatter cross section will approach 4%. If saturation occurs when the target is a perfect diffuse scatterer, in which the incident energy is randomly polarized and scattered uniformly over the hemisphere above the surface, then the limiting value corresponds to $0.5\rho_0$, where ρ_0 is the Fresnel reflectivity of the material. For our model, this would imply a real dielectric constant, ε', of 3.2. Analysis of the polarization properties of the Kilauea lava flows suggests that at most only 25% of the incident energy is depolarized [*Campbell et al.*, 1993], in which case our limiting value becomes $0.25\rho_0$, leading to a dielectric estimate of 5.4. Such estimates are consistent with the range in measured dielectric constants for these basaltic materials (see the appendix). Small changes in ρ_0 could be responsible for some of the scatter observed in the model fit, and a reflectivity term would be needed for application of these expressions to surfaces with significantly different values of ε'.

To test the utility of the radar scattering model, we first compared its predictions to the measured backscatter and roughness for each site at 68-cm wavelength. For the h_0 values, we extrapolated downward from a 1-m high-pass filtered profile value using the fractal dimensions presented in Table 1. Values of s were found by extrapolation from the 75-cm Allan deviation for each site (Figure 4, Table 1). The model predictions fit the 68-cm backscatter values relatively well in both cases (Figure 7). As expected, the fit is also very good at 24-cm wavelength, since we used these data to derive the model coefficients (Figure 8). The topographic profiles do not allow estimation of roughness at the 5.7-cm scale, so we

Figure 9. Normalized 5.7-cm HV radar data plotted against roughness parameters, with fit from model equations shown by solid line. (a) Backscatter power versus γ, with model fit from (8). (b) Backscatter power versus s, with model fit from (9).
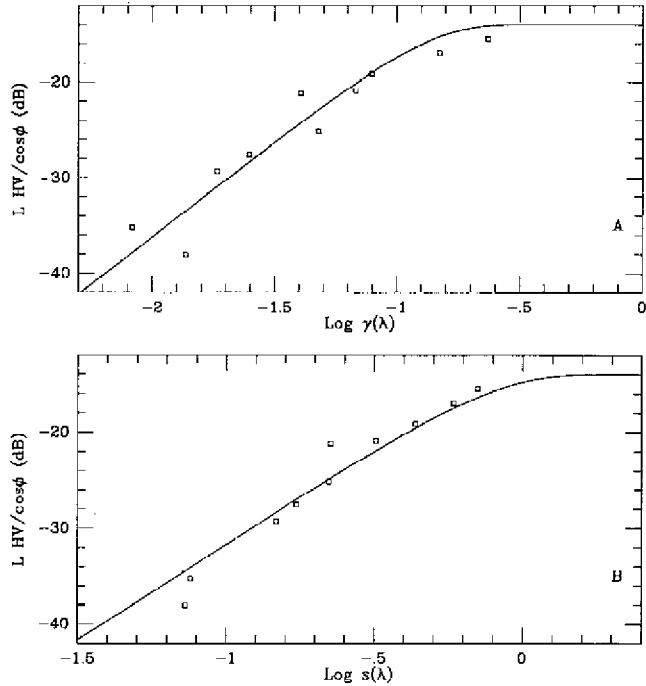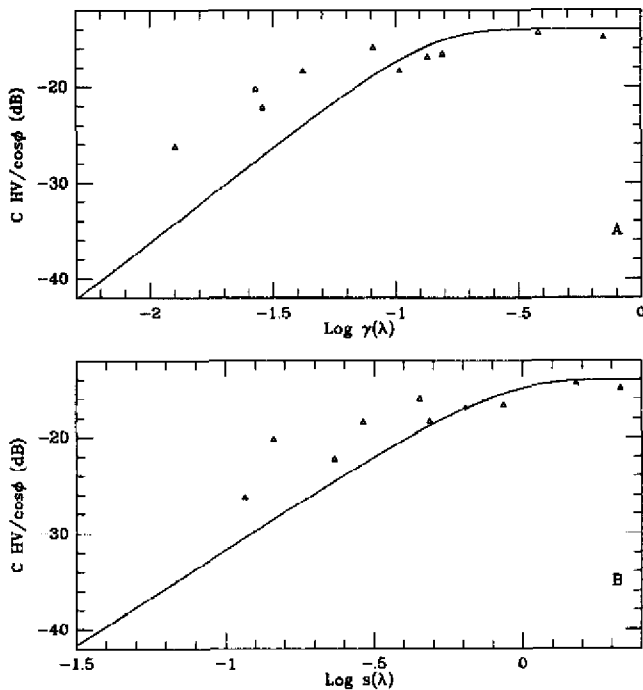
extrapolated downward for both h_0 and s values using the measured fractal dimensions. The model predictions agree with the data for rough terrain at 5.7 cm, but the correlation is poor for smoother surfaces viewed at this wavelength (Figure 9). This suggests that our topographic measurements, and the fractal dimension in particular, do not adequately characterize the small-scale texture of the flows, and that the error is worst when the overall roughness is small.

One explanation for the C band (5.7 cm) errors is that the physical processes responsible for the formation of small-scale roughness on the smoother flows differ from those which create the topography measured at 25-cm intervals, leading to errors in extrapolating correct values of h_0 or ν. For many pahoehoe lava flow surfaces, there is a ubiquitous covering of small glass chips which have weathered from the original chilled rind. The distribution of surface heights for these fragments is unrelated to the development of larger lava toes or billows, so we might expect a shift in behavior between these length scales. As we increase in size, the structure of

flow levees and ridges tends to reflect topographic and fluid pressure effects which are to some degree independent of the development of smaller surficial features, and again the self-affine behavior may change.

We tested this possibility using a limited set of high-resolution (5-cm) topographic profiles collected with a laser rangefinder (Figure 10) [Campbell and Garvin, 1993]. The characteristic parameters for these three sites are listed in Table 2, and it is evident that the largest discrepancy between fractal dimensions calculated from the two profile data sets occurs for the smoother pahoehoe surface (site 1). The value of ν(5 cm) derived for this site from the high-resolution profiles is nearly twice that extrapolated from the more coarsely sampled profile, which concurs with our observations of higher C band backscatter values (Figure 9). The measured and extrapolated values become progressively closer as roughness increases.

The functional form used in (8) and (9) has an interesting parallel to expressions derived for forward scattering from a rough plate. In this case, the reflectivity of the plate along the specular direction decreases exponentially with the square of the rms height for a fixed wavelength [Barrick and Peake, 1967; Beckmann and Spizzichino, 1963]. Our expression for diffuse scattering is thus the complement of the specular-lobe behavior. Peake and Oliver [1971] proposed that the energy lost from the specular lobe due to roughness would be randomly scattered in all directions, consistent with these results. This decline in specular echo (and increase in diffuse power) with roughness exhibits an asymptotic behavior similar to that found for our Hawaii observations, and the rollover in the curve was termed the Rayleigh breakpoint. Peake and Oliver [1971] and Schaber et al. [1976] analyzed radar data and rock distributions for a number of locations, and found that the breakpoint occurred at values of d/λ, where d is rock radius, from about 0.1 to 0.3. If these ratios are analogous to γ, then the breakpoint locations are in good agreement with the predictions of (8) (Figure 7). The link between diffuse echoes and the change in the specular lobe is not developed rigorously, but the parallels in their behavior raise interesting questions for modeling the physical scattering process.

These results demonstrate that the wavelength-scaled roughness, expressed as either the ratio of rms height at the wavelength scale to λ, or as the rms slope at the wavelength scale, is a useful parameter for predicting depolarized radar scatter from a rocky surface. Within the bounds of this limited sampling, the model matches both the roughness sensitivity and wavelength dependence of the radar echo from 5.7- to 68-cm wavelengths, and could presumably be extended to X band (3-cm) data as well. The discrepancies between radar-derived

Table 2. Values of the Fractal Dimension D, rms Height h_0 at 1 m Profile Length, and the Allan Deviation ν at 5-cm step sizes for Three Kilauea Sites

Site	D	h_0(1 m)	ν(5 cm)	ν_{ext}(5 cm)
1	1.86	1.08	1.33	0.75
6	1.61	4.27	3.85	2.54
7	1.73	6.13	7.33	8.01

Also shown is the value of ν(5 cm) extrapolated from the 25-cm profile data. Values of h_0 and ν are in units of centimeters. D values calculated from the slope of the variogram plot at horizontal scales <25 cm. Site numbers correspond to those in Table 1. Note the large discrepancy between extrapolated and measured Allan deviations for the smoother surfaces.
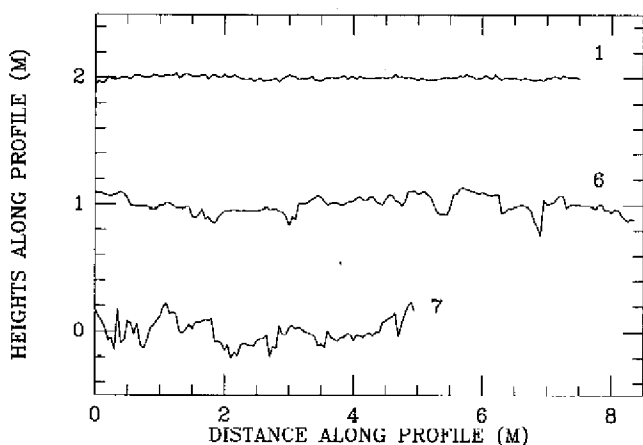
Figure 10. Topographic profiles for three sites on Kilauea collected at 5-cm horizontal spacing. Site numbers correspond to those on Figure 2. Profiles were detrended prior to analysis, and are offset for clarity.

values for h_0 or s at C band (5.7 cm) and those extrapolated from the topographic data are shown to be due to undersampling of small-scale topography by the 25-cm profiles. The lack of an extensive set of profiles at high spatial resolutions (i.e., 5 cm) precludes further testing of the derivation of fractal dimensions from the three-wavelength radar data, but such inferences could be made using the equations presented above.

Discussion

The lava surfaces chosen as test sites typically exhibit self-affine behavior over horizontal scales from 5 to 100 cm, and the degree to which a single fractal dimension defines the surface roughness across the scale range depends upon various contributing geologic processes. Where billows, toes, or plates exist, they tend to obey a single self-affine scaling relationship, but the presence of a weathered layer of glass on smoother surfaces creates an independent process whose scaling properties are different. This behavior was observed in both the field-measured topography and the radar backscatter data. The techniques discussed here for quantifying surface roughness with respect to the scale length of the

measurements should provide a means for topographic data collected by different groups to be compared.

It was shown that the diffuse component of radar scattering from rocky surfaces with minimal soil coverage can be related to the topographic roughness through a single parameter, and that the scaling of backcatter power with radar wavelength parallels that predicted from surface profiles. We also carried out a preliminary analysis of the polarized echo cross section (i.e., HH or VV), but found that no simple scaling relationship (similar to that found for the diffuse echo) can be defined. The small-facet echo is more complicated in its behavior with roughness, and it appears that a two-component probability density function is required to express the size and tilt of the various scattering elements. It may be possible to examine such models for Venus using the Magellan altimeter and synthetic aperture radar (SAR) data, which provide the near-nadir and oblique-angle coverage required to define the surface descriptive parameters. At any one wavelength and for a narrow range of incidence angles, the dependence of the HH return on roughness may be well represented by empirical fits, but these models must be treated with caution, in that they do not link the radar echo to a specific physical process or to the statistical properties of the surface.

In practice, the model equations can he used in a variety of ways. If HV echo values are available at a single wavelength, an estimate of the surface rms height or rms slope at the wavelength-scale can be made ((10) and (11)). If two or more wavelengths are collected, then the variability of terrain statistics with scale may be inferred. Differences in these derived values may indicate the types of varying small-scale structure we observed for the glass-covered pahoehoe flows. For Venus, we have depolarized circular images (LL polarization) from the Arecibo Observatory for about one-third of the surface, and a growing base of similar imagery for all of Mars. Since HV and LL echoes tend to differ only by a factor of 2 for rocky surfaces, the equations derived here can be used directly for inference of planetary surface roughness from the Arecibo data [Campbell et al., 1993].

Further work is required to define the reliability of the diffuse scattering model at smaller roughness scales, and additional collection of topography data at very high resolution (2-5 cm spacing) will help to test these results and our inferences about the changes in self-affine behavior for various surfaces. Extension of the studies to surfaces with a fine-grained surficial layer will widen the applicability of this

Table 3. Values of the Real Dielectric Constant Measured With a 24-cm Wavelength Coaxial Probe System

Site (Type)	$\varepsilon'_{surface}$	ε'_{core}	$\rho_{core},$ g/cm^3
1 (ML pah)	3.33	4.04	1.99
2 (ML pah)	3.22	5.02	2.16
3 (KI pah)	2.37	--	--
4 (KI pah)	2.47	--	--
5 (KI pah)	3.25	--	--
6 (KI pah)	3.24	--	--
7 (ML a'a)	--	5.61	2.26
8 (ML a'a)	--	7.35	2.68
9 (ML a'a)	--	6.76	2.32

Field-measured values for six pahoehoe flow surfaces are shown, with lab-measured values for density ρ and dielectric constant of core regions for comparison. Field measurement of a'a flows was not possible owing to the lack of smooth surface patches, so only lab results are shown here. Site numbers are not related to those discussed in text. ML designates Mauna Loa flows, KI designates Kilauea flows.

work, and may be of use in interpreting radar data for potential mantled areas on Venus and Mars.

Appendix: Measurement of Lava Flow Dielectric Constant

In an effort to constrain the bulk dielectric properties of the lava flows studied here, we measured the real component of the permittivity, ε', using a 24-cm wavelength coaxial-probe system provided by JPL. This system is capable of also estimating the imaginary portion of the dielectric constant, ε'', but we found in practice that these values were questionable. In the field, the probe must make solid contact with a relatively smooth 3- to 5-cm diameter area of the lava, which restricted its application to pahoehoe surfaces with intact glassy rinds. Rougher a'a flows and weathered pahoehoe surfaces yielded poor results.

We studied six pahoehoe flows from Mauna Loa and Kilauea, and the resulting measurements are shown in Table 3. Each tabulated value is the average of 15-20 separate readings on the lava surface. The mean value for all six flows is 2.98, which seems low given the rocky nature of these lavas. The field measurements, however, sample primarily the upper layer of the flow surface, which is typically characterized by a higher vesicularity (lower density) than the central flow core. Samples of some Mauna Loa flows (pahoehoe and a'a) were sawed to obtain a smooth face, and dried in an oven for 24 hours to remove any water. Areas within the core area of the pahoehoe flows had values of ε' from 4 to 5, while more dense a'a flow centers reached values of 7.35. We thus conclude that (1) differences in dielectric constant between and within the various lava flows are dominated by bulk density variations, consistent with other lab studies of basalts [Ulaby et al., 1988]; (2) the upper few centimeters of many pahoehoe flows tend to be less dense than the inner core, leading to a slightly lower Fresnel reflection coefficient.

References

Arvidson, R., M. Shepard, E. Guiness, S. Petroy, J. Plaut, D. Evans, T. Farr, R. Greeley, N. Lancaster, and L. Gaddis, Characterization of lava flow degradation in the Pisgah and Cima volcanic fields, California, using Landsat Thematic Mapper and AIRSAR data, Geol. Soc. Am. Bull., 105, 175-188, 1993.

Barrick, D.E., and W.H. Peake, Scattering from surfaces with different roughness scales: Analysis and interpretation, Rep. 1388-26, Ohio State Univ. Electrosci. Lab., Columbus, 1967.

Beckmann, P., and A. Spizzichino, The Scattering of Electromagnetic Waves From Rough Surfaces, Pergamon, New York, 1963.

Benallegue, M., O. Taconet, D. Vidal-Madjar, and M. Normand, The use of radar backscattering signals for measuring soil moisture and surface roughness, Remote Sens. Environ., 53, 61-68, 1995.

Campbell, B.A., and J.B. Garvin, Lava flow topographic measurements for radar data analysis, Geophys. Res. Lett., 20, 831-834, 1993.

Campbell, B.A., S.H. Zisk, and P.J. Mouginis-Mark, A quad-pol radar scattering model for use in remote sensing of lava flow morphology, Remote Sens. Environ., 30, 227-237, 1989.

Campbell, B.A., R.E. Arvidson, and M.K. Shepard, Radar polarization properties of volcanic and playa surfaces: Applications to terrestrial remote sensing and Venus data interpretation, J. Geophys. Res., 98, 17,099-17,113, 1993.

Evans, D.L., T.G. Farr, J.P. Ford, T.W. Thompson, and C.L. Werner, Multipolarization radar images for geologic mapping and vegetation discrimination, IEEE Geosci. Remote Sens., GE-24, 246-257, 1986.

Farr, T.G., Microtopographic evolution of lava flows at Cima Volcanic Field, Mojave Desert, California, J. Geophys. Res., 97, 15,171-15,179, 1992.

Freeman, A., J.J. van Zyl, J.D. Klein, H.A. Zebker, and Y. Shen, Calibration of Stokes and scattering matrix format polarimetric SAR data, IEEE Geosci. Remote Sens., 30, 531-539, 1992.

Gaddis, L.R., Lava flow characterization at Pisgah volcanic field, California, with multiparameter imaging radar, Geol. Soc. Am. Bull., 104, 695-703, 1992.

Gaddis, L.R., Evaluation of an empirical radar backscatter model for predicting backscatter characteristics of geologic units at Pisgah volcanic field, California, Geophys. Res. Letters, 21, 1803-1806, 1994.

Gaddis, L.R., P.J. Mouginis-Mark, and J.N. Hayashi, Lava flow surface textures: SIR-B radar image texture, field observations, and terrain measurements, Photogramm. Eng. Remote Sens., 56, 211-224, 1990.

Hagfors, T., Backscattering from an undulating surface with applications to radar returns from the Moon, J. Geophys. Res., 69, 3779-3784, 1964.

Hagfors, T., A study of the depolarization of lunar radar echoes, Radio Sci., 2, 445-465, 1967.

Hapke, B., Bidirectional reflectance spectroscopy, 3, Correction for macroscopic roughness, Icarus, 59, 41-59, 1984.

McCollom, T.M., and B.M. Jakosky, Interpretation of planetary radar observations: The relationship between actual and inferred slope distributions, J. Geophys. Res., 98, 1173-1184, 1993.

Oh, Y., K. Sarabandi, and F.T. Ulaby, An empirical model and an inversion technique for radar scattering from bare soil surfaces, IEEE Trans. Geosci. Remote Sens., 30, 370-381, 1992.

Peake, W.H., and T.L. Oliver, The response of terrestrial surfaces at microwave frequencies, Tech. Rep. AFAL-TR-70-301, 255 pp., Ohio State Univ., Columbus, 1971.

Pettengill, G.H., P.G. Ford, and B.D. Chapman, Venus: Surface electromagnetic properties, J. Geophys. Res., 93, 14,881-14,892, 1988.

Rowland, S.K., and G.P.L. Walker, Pahoehoe and a'a in Hawaii: Volumetric flow rate controls the lava structure, Bull. Volcanol., 52, 615-628, 1990.

Schaber, G.G., G.L. Berlin, and W.E. Brown, Variations in surface roughness within Death Valley, California: Geologic evaluation of 25-cm-wavelength radar images, Geol. Soc. Am. Bull., 87, 29-41, 1976.

Schaber, G.G., C. Elachi, and T.G. Farr, Remote sensing of SP mountain and SP lava flow in North-central Arizona, Remote Sens. Environ., 9, 149-170, 1980.

Shepard, M.K., R.A. Brackett, and R.E. Arvidson, Self-affine (fractal) topography: Surface parameterization and radar scattering, J. Geophys. Res., 100, 11,709-11,718, 1995.

Smith, B.G., Geometrical shadowing of a random rough surface, IEEE Trans. Antennas Propag., AP-15, 668-671, 1967.

Ulaby, F.T., R.K. Moore, and A.K. Fung, Microwave Remote Sensing, Addison-Wesley, Reading, Mass., 1982.

Ulaby, F.T., T. Bengal, J. East, M.C. Dobson, J. Garvin, and D. Evans, Microwave dielectric spectrum of rocks, Rep. 23817-1-T, 81 pp., Univ. of Mich. Radiat. Lab., Ann Arbor, 1988.

van Zyl, J.J., Calibration of polarimetric radar images using only image parameters and trihedral corner reflector responses, IEEE Trans. Geosci. Remote Sens., 28, 337-348, 1990.

van Zyl, J.J., C.F. Burnette, and T.G. Farr, Inference of surface power spectra from inversion of multifrequency polarimetric radar data, Geophys. Res. Lett., 18, 1787-1790, 1991.

Wagner, R.J., Shadowing of randomly rough surfaces, J. Acoust. Soc. Am., 41, 138-147, 1966.

B.A. Campbell, MRC 315, Smithsonian Institution, Washington, DC 20560. (e-mail: campbell@ceps.nasm.edu)

M.K. Shepard, Department of Geography and Earth Science, Bloomsburg University, Bloomsburg, PA 17815. (e-mail: shepard@planetx.bloomu.edu)